Supplementary materials for

Thermal Decomposition of Nano Al-based Energetic Composites with Fluorinated Energetic Polyurethane Binders: Experimental and Theoretical Understandings for the Enhanced Combustion and Energetic Performance

Gang Tang,[a] He Wang,[b] Chunyan Chen,[c] Yabei Xu,[b] Dongping Chen,[*b] Dongli Wang,[a] Yunjun Luo,[*a, d] Xiaoyu Li[*a, d, e]

[a] School of Materials Science and Engineering, Beijing Institute of Technology, Beijing, 100081, China

[b] State Key Lab of Explosion Science and Technology, Beijing Institute of Technology, Beijing, 100081, China

[c] Xi'an Modern Chemistry Research Institute, Xi'an, 710065, China

[d] Key Laboratory of High Energy Density Materials, Ministry of Education, Beijing Institute of Technology, Beijing, 100081, China

[e] Experimental Center of Advanced Materials, Beijing Institute of Technology, Beijing 100081, China

Corresponding author

E-mail: dc516@bit.edu.cn. (D.P. C.)

E-mail: yjluo@bit.edu.cn. (Y.J. L.)

E-mail: xiaoyuli@bit.edu.cn. (X.Y. L.)

Contents

1. Supplementary Discussions

Chemical Reaction Neural Network Modeling

The reaction equation of the FPUs/AlNPs thermal decomposition is defined as follows:

$$v_1'\left[\text{FPUs/AlNPs}\right]+v_2'S_2+\cdots+v_n'S_n \rightarrow v_1''\left[\text{FPUs/AlNPs}\right]+v_2''S_2+\cdots+v_n''S_n \quad \text{* MERGEFORMAT (1)}$$

where v_i' and v_i" correspond to the stoichiometric coefficients of reactants and products, respectively; S_n refers to the intermediates and products, where S_n might represent multiple substances. According to the mass action law and Arrhenius law, the above reaction rate can be written as:

$$r=\left[\text{FPUs/AlNPs}\right]^{v_1'}\left[S_2\right]^{v_2'}\cdots\left[S_n\right]^{v_n'}\times AT^n\exp\left(-E_a/RT\right) \quad \text{* MERGEFORMAT (2)}$$

$$r=\exp\begin{pmatrix}v_1'\ln[\text{FPUs/AlNPs}]+v_2'\ln\left[S_2\right]+\cdots+v_n'\ln\left[S_n\right]\\+\ln A+n\ln T-E_a/RT\end{pmatrix}. \quad \text{* MERGEFORMAT (3)}$$

where the parameters A, n and E_a represent the pre-exponential factor, the nonexponential temperature-dependent factor, and the activation energy, respectively. The formation rate of each intermediate and product can be further expressed as:

$$\frac{d[FPUs/AlNPs]}{dt}=[\dot{FPUs/AlNPs}]=-v_1'r+v_1''r$$

$$\frac{d[S_2]}{dt}=[\dot{S}_2]=-v_2'r+v_2''r$$

$$\frac{d[S_2]}{dt}=[\dot{S}_3]=-v_3'r+v_3''r \quad (4)$$

$$\vdots$$

$$\frac{d[S_n]}{dt} = [\dot{S}_n] = -v_n'r + v_n''r$$

The single-step reaction and the multistep reaction CRNN network are illustrated in Fig. S1. The reaction in Eq. (1) is expressed as a neuron, as shown in Fig. S1(a), and the formula is expressed as $y = \sigma(wx + b)$, where x is the input of the neuron, representing the mass concentration and temperature of each component in the system; y is the output, representing the reaction rate of each component in the system; w is the weight, which refers to the activation energy in the Arrhenius equation and the stoichiometric coefficient in the reaction equation; b is the deviation, corresponding to the pre-exponential factor A in the Arrhenius formula; and σ is the nonlinear activation function, which can avoid overfitting. Overall, the thermal decomposition of FPUs/AlNPs involves multiple steps, and individual neurons can be stacked to form a neural network with one hidden layer, as shown in Fig. S1(b). The number of nodes in the hidden layer of the neural network equals the number of reactions in the CRNN model.

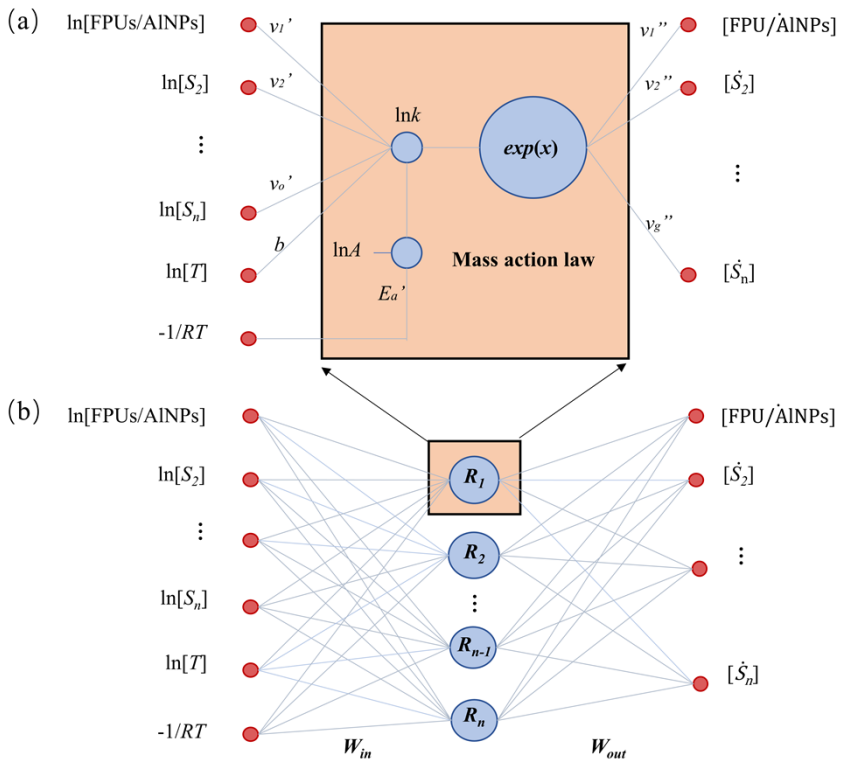

Fig. S1. Schematic illustrations of a CRNN network (a) for a single-step reaction, and (b) for multistep reactions.

The loss function of the neural network is defined as the mean absolute error (MAE) between the mass fraction of thermo gravimetric experiments (TG) and the mass fraction predicted by the model:

$$\text{Loss} = \text{MAE}(m_{\text{res}}^{\text{exp}} - m_{\text{res}}^{\text{CRNN}}) \qquad \text{* MERGEFORMAT} \tag{4}$$

where $m_{\text{res}}^{\text{exp}}$ and $m_{\text{res}}^{\text{CRNN}}$ are the mass fractions of the remaining substances in TG experiments and the neural network model, respectively. The following constraints are subsequently added to the CRNN model for FPUs/AlNPs decomposition: (1) FPUs/AlNPs only exist in the reactants; (2) mass stoichiometry balancing; and (3) E_a and ln$A$ are in the range of 0~300 kJ/mol and -20 to 50, respectively.

The kinetic model of FPU-98-40 was deduced using the CRNN model by assuming

different model sizes. Three kinetic models of FPUs/AlNPs are inferred as the "3-3", "4-4" and "5-5" models. The model training was performed on three data sets (10, 20 and 40 K/min), and the data set of 30 K/min was used for validation to avoid overfitting. Fig. S6 shows the computational losses of the 5-5 model with five reactions (number of reactions, *nr*) and five species (number of species, *ns*) during the interactions of CRNN training and validation. In Fig. S2, the loss in the training set drops rapidly in the first ~500 iterations reaching an error of less than 0.1. To ensure training accuracy, the model was trained for 5000 iterations. After 5000 iterations, the prediction error of the model for TG experiments fluctuated at ~0.05.

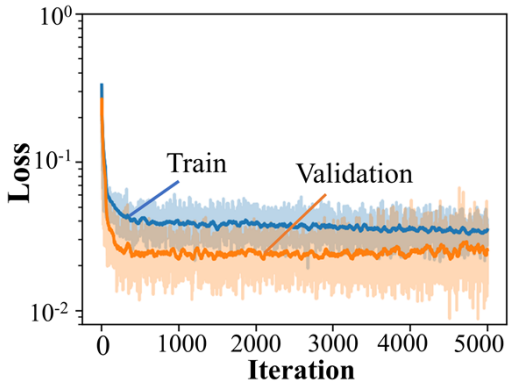

Fig. S2. The errors of the CRNN model in the training set and validation set (*ns*=5, *nr*=5).

Table S1. Reaction mechanisms in the 3-3 and 4-4 models.

Model	Index	Reaction	E_a (kJ/mol)	n	ln$A$
3-3[a]	R_1	1FPUs/AlNPs → 1 S_2	153.89	0	4.81
	R_2	1FPUs/AlNPs → 1 S_2	101.42	0.11	8.32
4-4	R_1	10FPUs/AlNPs → 6 S_2 + 3 S_3 + 1 S_4	24.68	0.02	8.88
	R_2	1 S_3 → 1 S_2	50.76	0.84	5.11
	R_3	5 S_2 → 6 S_3	40.91	0.13	6.06
	R_4	2 S_2 + 3 S_3 → 5 S_4	30.76	0.13	6.64

[a] The stochiometric coefficients in R_3 are all zero, and thus R_3 is neglected in the 3-3 model.

Table S1 shows the reaction mechanism of the 3-3 and 4-4 models. Fig. S3 includes the predicted thermal decomposition of FPUs/AlNPS at four different heating rates using the 3-3 and 4-4 models. The predicted mass loss of the 3-3 model deviates significantly from the experimental value, with an overall error of 0.21, indicating a

failure of training owing to the small model size. The predicted error of the 4-4 model is 0.06, and the predicted value only deviates slightly from the experimental curve at a heating rate of 30 K/min. Further increasing the model size, we find that the 5-5 model could well reproduce the experimental TG curves with an overall error of 0.03. Consequently, we only consider the 5-5 model in the discussion to reveal the reaction mechanisms of FPUs/AlNPS decomposition.

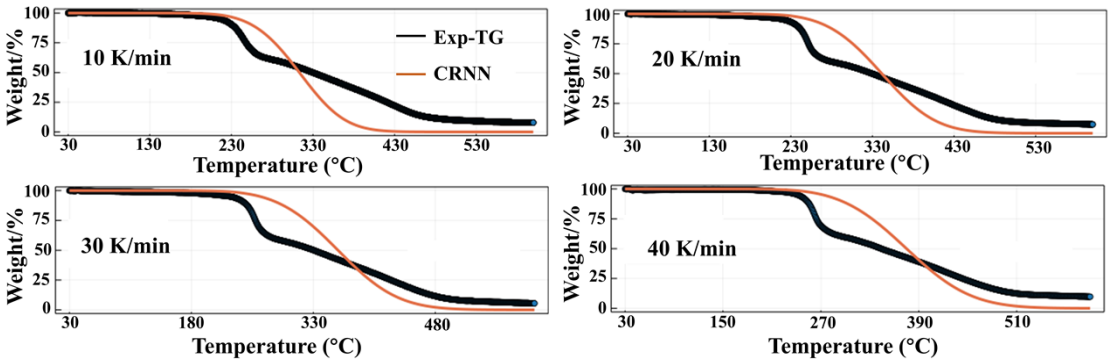

(a)*ns*=3, *nr*=3

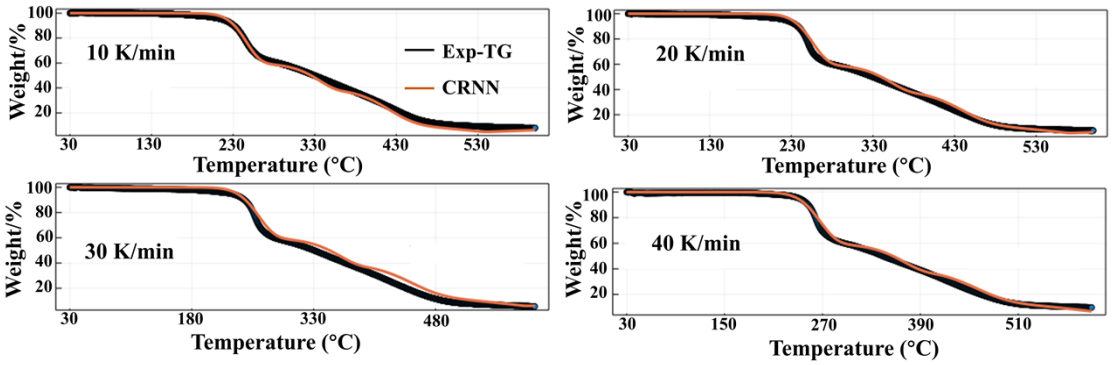

(b)*ns*=4, *nr*=4

Fig. S3. The TG curves predicted by the CRNN models (red line) and experimental results (black line).

Fig. S4 illustrates the rate of each reaction as a function of temperature in the 5-5 model, and the specific values are shown in Table S2. The reaction rates are very

sensitive to temperature. Among all five reactions, R_2 has the highest rate constant; R_2 is 1-2 orders of magnitude higher than that of R_3. As R_2 and R_3 are competing reactions for the decomposition of S_4, R_2 prevails because of the higher rate constant. Similarly, R_5 controls the reaction between S_2 and S_3, and R_4 can be neglected from the reaction mechanism.

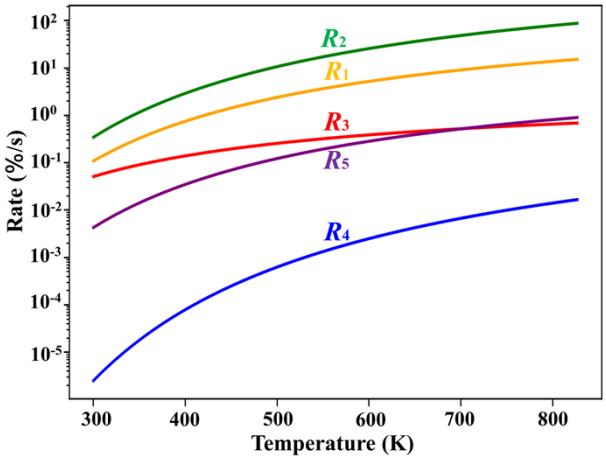

Fig. S4. Comparison of rate constants in 5-5 model.

Table S2. Rate constants of all five reactions in 5-5 model[a]

Temperature (K)	300	400	500	600	700	800
R_1	0.11	0.74	2.36	5.13	8.95	13.61
R_2	0.34	2.86	10.50	25.27	47.72	77.39
R_3	0.05	0.14	0.25	0.38	0.51	0.64
R_4	0.00	0.00	0.00	0.00	0.01	0.01
R_5	0.00	0.03	0.12	0.28	0.51	0.80

[a] The unit of rate constant in each reaction is reported as mass percentage per second (e.g. %/s).

2. Supplementary Figure

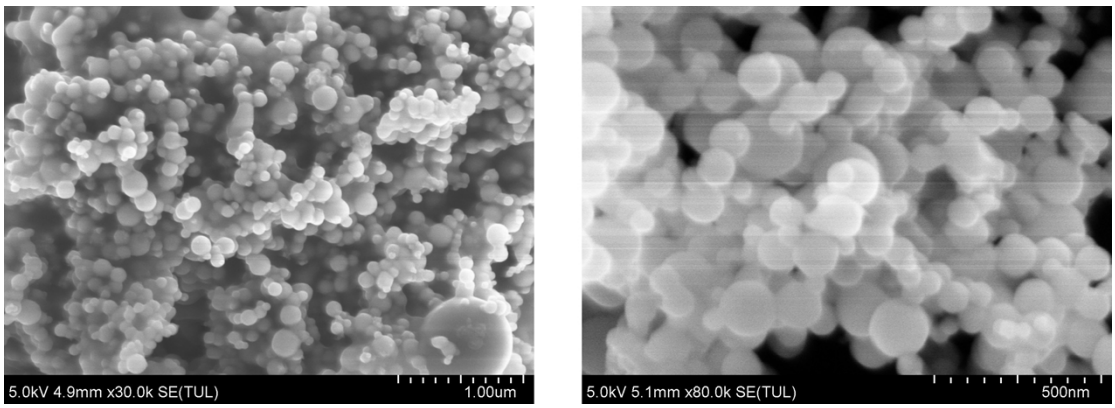

Fig. S5 SEM images of AlNPs.

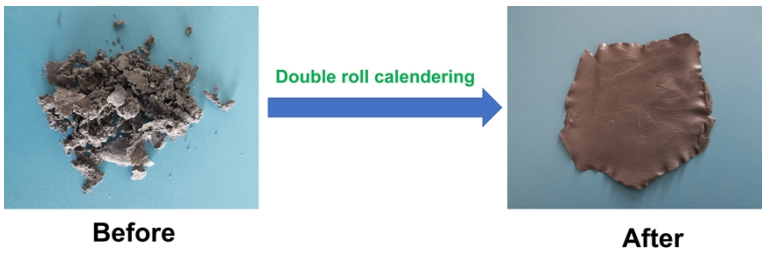

Fig. S6 The before and after photograph of FPUs/AlNPs composites by double roll calendering

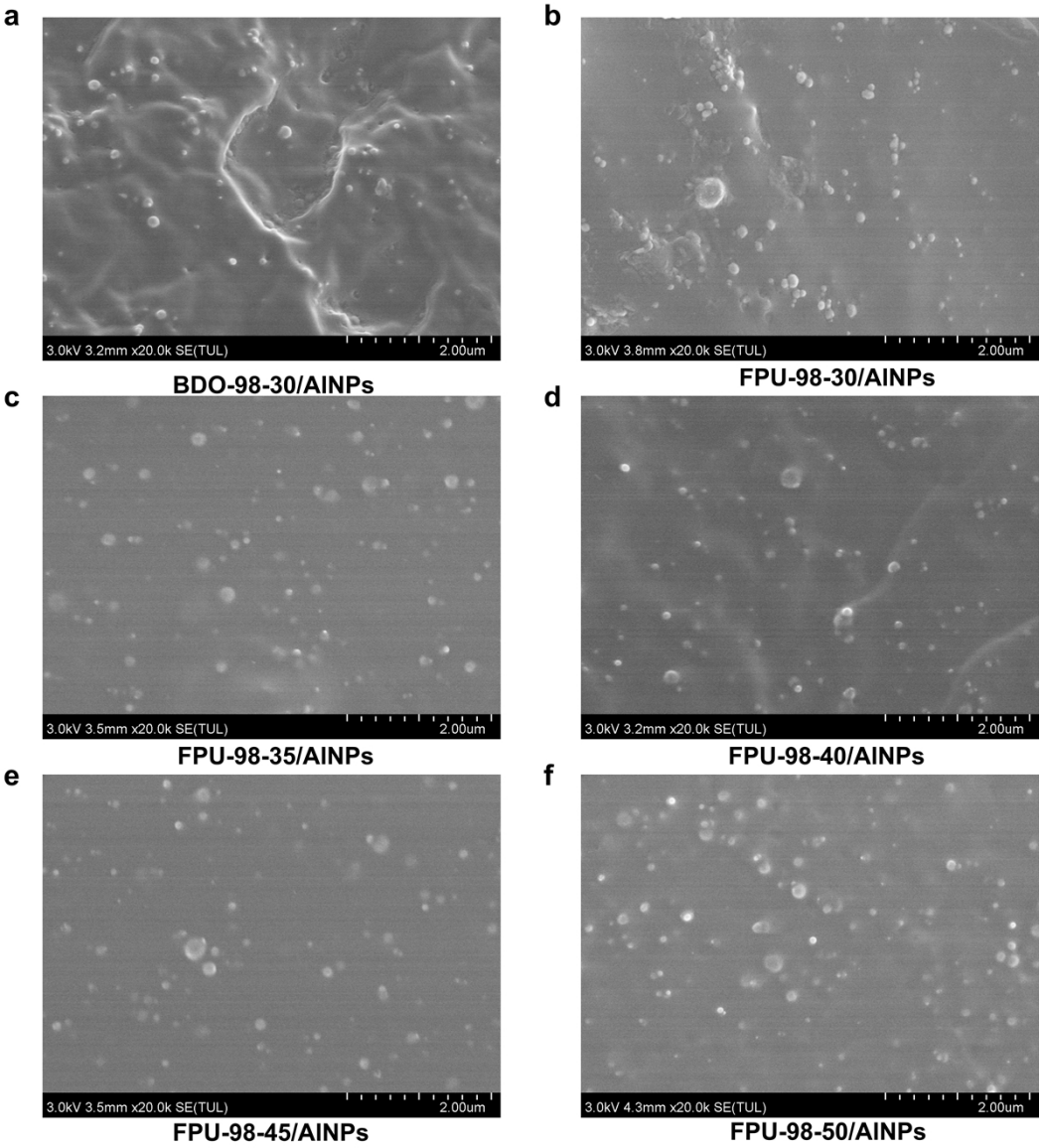

Fig. S7 SEM images of the fractured surface for the ETPUEs/AlNPs composites.

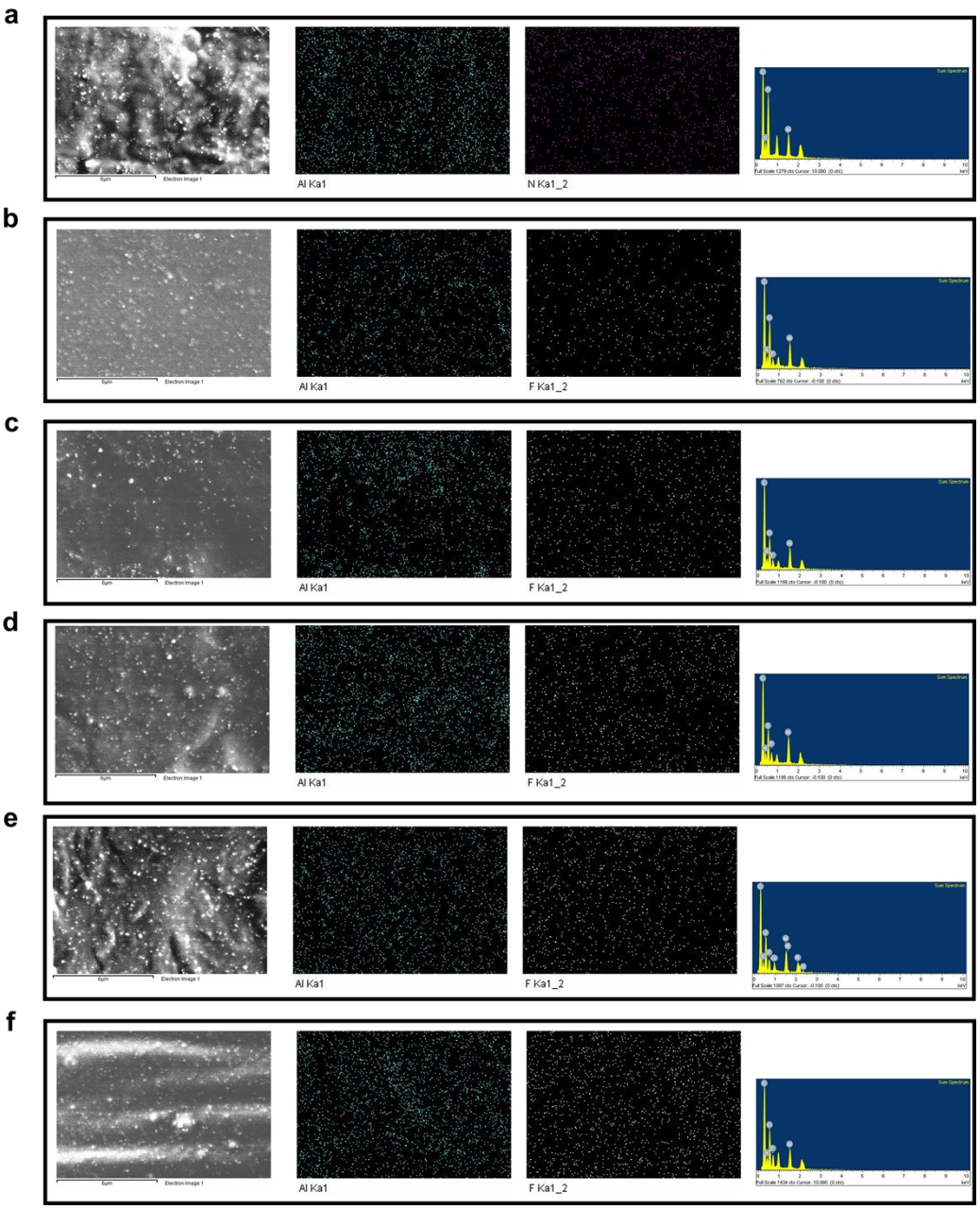

Fig. S8 SEM-EDS analysis results of the fractured surface for the (a) BDO-98-30/AlNPs, (b) FPU-98-30/AlNPs, (c) FPU-98-35/AlNPs, (d) FPU-98-40/AlNPs, (e) FPU-98-45/AlNPs and (f) FPU-98-50/AlNPs composites.

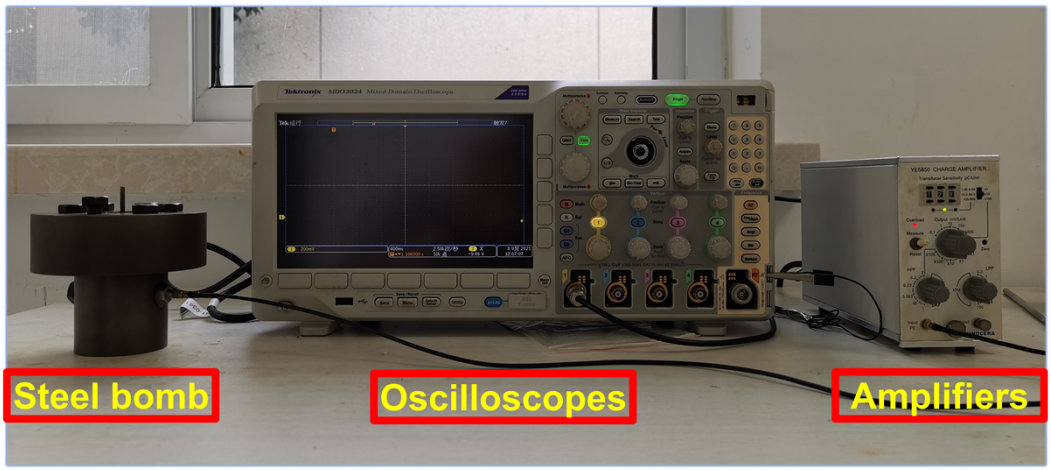

Fig. S9 The photograph of the dynamic pressure characteristics instrument.